Mapping physicochemical surface modifications of flame-treated polypropylene

S. Farris[1*], S. Pozzoli[1], S. La Vecchia[1], P. Biagioni[2], C. L. Bianchi[3], L. Piergiovanni[1]

[1]DeFENS, Department of Food, Environmental and Nutritional Science, Packaging Division – University of Milan, Via Celoria 2, 20133 Milan, Italy
[2]Dipartimento di fisica and CNISM, Politecnico di Milano, Piazza L. da Vinci 32, 20133 Milano, Italy
[3]Department of Chemistry, University of Milan, Via Golgi 19, I, 20133 Milano, Italy

Abstract. The aim of this work was to investigate how the surface morphology of polypropylene (PP) is influenced by the surface activation mediated by a flame obtained using a mixture of air and propane under fuel-lean (equivalence ratio φ = 0.98) conditions. Morphological changes observed on flamed samples with smooth (S), medium (M), and high (H) degree of surface roughness were attributed to the combined effect of a chemical mechanism (agglomeration and ordering of partially oxidized intermediate-molecular-weight material) with a physical mechanism (flattening of the original roughness by the flame's high temperature). After two treatments, the different behavior of the samples in terms of wettability was totally reset, which made an impressive surface energy of ~43 mJ·m^{-2} possible, which is typical of more hydrophilic polymers (e.g., polyethylene terephthalate – PET). In particular, the polar component was increased from 1.21, 0.08, and 0.32 mJ·m^{-2} (untreated samples) to 10.95, 11.20, and 11.17 mJ·m^{-2} for the flamed samples S, M, and H, respectively, an increase attributed to the insertion of polar functional groups (hydroxyl and carbonyl) on the C–C backbone, as demonstrated by the X-ray photoelectron spectroscopy results.

Keywords: coatings, flame treatment, polypropylene, surface activation, wettability

1. Introduction

Since its discovery in 1954 [1], polypropylene (PP) has become increasingly important for fabricating the materials, objects, goods, and commodities of everyday life [2]. The reason for this long-lasting growth lies mainly in the properties of PP, such as chemical resistance to most organic solvents, fatigue resistance, high clarity, very good water vapor barrier properties, compatibility with many processing techniques, low density, easy recyclability and – not least of all – moderate cost. Although PP's inability to stand thermal stresses and its poor gas barrier properties may hinder its use for certain applications, the major hurdle is probably its surface properties. Like any polyolefin, PP exhibits low surface free energy

values (~28 mJ·m^{-2}), which are due in essence to its inherent hydrophobicity. This is reflected primarily in the high recalcitrance of polypropylene surfaces toward the deposition of substances (e.g., liquids) with a high polar component: it totally frustrates the establishment of either interatomic or intermolecular interactions at the interface [3]. This repulsion dramatically affects all technical processes where wettability and improved adhesion are required. Printability, lamination, and anti-fog properties, as well as the processability, convertibility, recyclability, and biodegradability of the final materials depend strongly on the possibility of enhancing the polypropylene substrate's surface properties. Consequently, enhancing the surface activation of poly-

propylene (and, more generally, of polyolefins) has attracted (and still does) worldwide interest both in academia and in industrial research [4].

With reference to the source of activation (and not to the type of modification induced on the polymer surface) the main routes used to improve the surface energy of polyolefins can be grouped into chemical and physical methods [5]. Physical methods, however, are the most extensively used because they allow the provision of more precise surface modification without requiring rigorous process control, and because, involving no chemical reagents and therefore no disposal of waste liquids, they are environmentally safe and clean processes [6]. Among the wide spectrum of physical methods currently available for the surface modification of plastics (flame [7], corona discharge [8], UV [9], gamma-ray [10], electron beam [11], ion beam [12], plasma [13], and laser treatments [14]), flame treatment and corona discharge are the most widespread, especially in particular sectors such as packaging and automotive, which has primarily been ascribed to the lower cost of these methods. It has been pointed out, however, that flame treatment is probably the most suited for the surface activation of polyolefins and, within this category, polypropylene [15]. Nevertheless, the great potential involved in the flame treatment was underexploited until 1980s [16], when remarkable innovations at both the technical (e.g., the introduction of the polarized flame) and the safety level renewed interest in this method. Correspondingly, the acquisition of new powerful techniques such as optical contact angle (OCA) [17], atomic force microscopy (AFM) [18], and X-ray photoelectron spectroscopy (XPS) [19–21] prompted a fervid scientific activity, as demonstrated by the number of scientific papers in this area [16, 22–24].

At the present time, interest toward flame treatment relies mainly on the innovations expected in many areas for the next years. New developments will take place according to specific trends, among which the environmental aspect seems to be one of the main driving forces. Many companies are progressively looking for new, high-performance materials that are perceived by consumers as environmentally friendly and safe. Legislation also forces new trends [25]. Since water-based coatings are expected to play a major role in the future, the flame treatment technique may play a pivotal role in dictating the success of their deposition on PP. However, to make

the flame treatment effective towards high-recalcitrant substrates, knowing the basic principles underlying the overall process is of utmost importance [26]. This in turn will enable optimization of the main process variables to pinpoint the best operating conditions for any specific application [27]. A key factor possibly influencing the efficacy of the flame treatment is the sample's topography. There is, however, a lack of information on how surface roughness affects the activation of polypropylene substrates mediated by a flame [26].

This work was aimed at filling this gap by investigating how the substrate topography influenced the flame treatment's overall effect, by taking into account both the physical and the chemical changes that the process induced. To this end, the benefits possibly linked to changes in the surface roughness of polypropylene samples in terms of surface energy were quantitatively described. The effect of an increasing number of sequential treatments was also discussed. This was accomplished by OCA and AFM techniques, whereas XPS analysis was used to gather detailed information on the chemical changes induced by the flame.

2. Experimental section
2.1. Polymer samples
Square plaques 40 mm wide and 3 mm thick were used throughout the experiments. They were produced by injection-molding, starting from PP pellets (Moplen RP340R, Basell Polyolefins srl, Ferrara, Italy; nucleated heterophasic random copolymer, melt flow index according to ISO 1133: 25 g/10 min, density according to ISO 1183: 0.905 g/cm^3, melting range = 140–163°C), fed into the heated barrel, mixed through a screw, and injected into a multiple-cavity mold (each cavity having identical geometry). The mold is then held under pressure until the material cools and hardens, after which the mold is opened and the part is removed. To produce plaques with different surface topographies, interchangeable molds with front panel of three different roughness degrees (perfect smoothness – S, medium roughness – M, and high roughness – H) were used. Unlike usual injection-molding manufacturing operations, the use of any release agent (which helps in the detachment of the object from the mold) was avoided, to prevent potential interference with the contact angle measurements. Injection-molded (OCSA spa, Creazzo, Italy) PP

(Moplen RP340R, nucleated heterophasic random copolymer, Basell Polyolefins srl, Ferrara, Italy) square plaques (40 mm wide, 3 mm thick) with different roughness degrees (perfect smoothness – S, medium roughness – M, and high roughness – H) were used in this work. The different roughness was achieved using interchangeable plates with a different surface morphology during the injection-molding process.

2.2. Surface modification apparatus and procedures

Flame treatment was performed with pilot-plant-flaming equipment built within the laboratories at the Packaging Division of DeFENS (University of Milan). An explanatory scheme is shown in Figure 1. It basically consists of a feeding system (fuel and oxidizer cylinders) connected to a fuel/oxidizer mix generator (mod. EI-080, esseCI srl, Narni, Italy); two single-flow-tube universal rotameters (ASA, Sesto S. Giovanni, Italy), one for the oxidizer (mod. 1901, flow range$_{air}$ 85–850 L·h^{-1}, 1013 mbar, 20°C), one for the fuel (flow range$_{air}$ 4–115 L·h^{-1}, 1013 mbar, 20°C); a pressure gauge; an in-line mixture sampling device; a 100 mm×20 mm ribbon burner with no-return flame valves (esseCI srl, Narni, Italy); and a sample holder composed by an aluminum rotating plate and a speed-regulating automatic
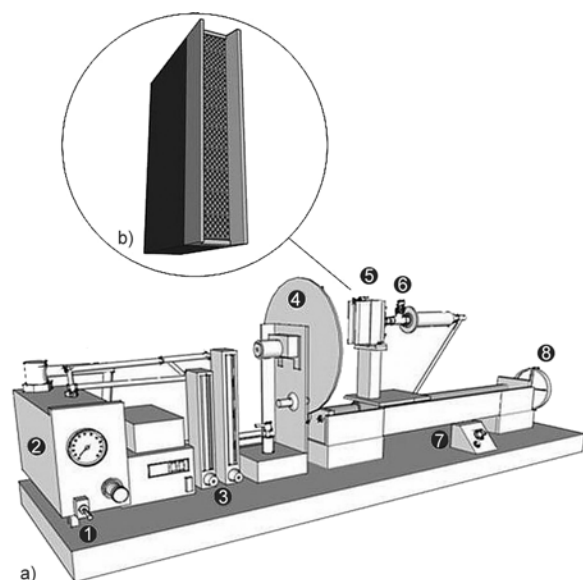

Figure 1. (a) Schematic representation of the flame treatment apparatus: 1 – manual start; 2 – gas/air mixer; 3 – gas and air flow rotameters; 4 – rotating sample holder; 5 – ribbon burner; 6 – gas/air mixture sampling valve; 7 – sample holder speed control (relay); 8 – flame-to-sample gap manual adjuster. (b) Magnification of the ribbon burner.

device. Ignition of the flame was accomplished by an electric spark.

The configuration of the flaming treatment made it possible to adjust the main process variables, such as the fuel/oxidizer ratio, the mixture flow, the flame/surface gap (i.e., the distance between the tips of the luminous flame cones and polyolefin surface), the sample's time of exposure to the flame, and the number of sequential treatments. The oxidizer used in this work was compressed air (Siad, Osio Sopra, Italy), whereas the fuel was commercial-grade liquid propane (GPL, Sarpomsrl, Trecate, Italy) with an average density of 0.5174 kg·L^{-1} and average heat content of 93.1 kJ·L^{-1} (2500 BTU·ft^{-3}). The average volumetric composition of GPL is as follows: C3 hydrocarbons, 93.9%; C4 hydrocarbons, 5.8%; C2 hydrocarbons, 0.3%; total sulfur content, 8.0 mg·kg^{-1}; water content, 18 mg·kg^{-1}.

Flame treatments were performed by a propane/air equivalence ratio of 0.98. According to Equation (1), the equivalence ratio (φ) is defined as the actual mass gas/air ratio used during treatment divided by the stoichiometric fuel-to-oxidizer ratio [28]:

$$\varphi = \frac{\dfrac{m_{fuel}}{m_{oxidizer}}}{\left(\dfrac{m_{fuel}}{m_{oxidizer}}\right)_{stoichiometric}} \tag{1}$$

The value selected in this work ($\varphi = 0.98$) accounts for the better performance of oxidizing flames ($\varphi < 1$) compared with both stoichiometric ($\varphi = 1$) and fuel-rich ($\varphi > 1$) flames [29–31]. The equivalence ratio value was continuously monitored throughout the experiments by the sampling of a constant amount (30 µL) of the mixture, and its analysis by a gas-chromatograph coupled with a flame ionization detector (GC-FID PR 2100 Perichrom, Saulx les Chartreux, France).The C$_3$H$_8$ was separated from the other components in the mixtures by a 80/100 mesh Porapak® T packed column (182.88 cm length; 3.175 cm external diameter; 2.159 cm internal diameter). The column inlet was set in splitless mode at 105°C and 75 kP. The column temperature was isothermal at 150°C, with a helium carrier flow of 38 mL·min^{-1}. The FID system (260°C, 75 kP, 10^{-10} A/mV gain) was fuelled with pure oxygen at 420 mL·min^{-1} and hydrogen at 30 mL·min^{-1}. Finally, an equivalence ratio of 0.98 was achieved by a flow setting of 700 and 74.5 L·h^{-1} for compressed air and

propane, at an outlet pressure of ~5.5 and ~2.8 bar, respectively.

Additional operating conditions were: substrate-to-flame distance, 5.0 mm; flame contact time, 0.05 s. To assess the influence of the number of flame treatments, polypropylene surfaces were exposed to 1 or 2 sequential treatments; in the latter case, between two flame passes, the samples were allowed to rest for 10 s for the polymer's surface to cool down. The flame power, i.e. the product of the volume of fuel burned per unit time (80 L·h^{-1} in our work) and the heat content of the fuel (93.1 kJ·L^{-1}) was approximately equal to 6938 kJ·h^{-1}, corresponding to ~1927 W. Since the effective burning surface (namely the sum of the area of the 129 holes of the burner grid ejecting the flame cones) amounted to 3.3 cm^2, the unit flame power was equal to ~584 W cm^{-2}, which yielded tip-luminous cones that were approximately 3 mm tall.

2.3. Physicochemical characterization

Contact angle measurements

Surface activation of polypropylene samples was firstly assessed by an optical contact angle apparatus (OCA 15 Plus – Data Physics Instruments GmbH, Filderstadt, Germany) equipped with a video measuring system with high-resolution CCD camera and a high-performance digitizing adapter. The software SCA 20 (Data Physics Instruments GmbH, Filderstadt, Germany) was used for data acquisition. For flamed samples, each contact angle measurement was performed immediately (~10 s) after the treatment. Rectangular (5 cm×2 cm) polypropylene samples (untreated and flame-treated) were fixed throughout the analysis by means of a special sample holder with parallel clamping jaws. The contact angle (θ [°]) of both water (Milli-Q water, 18.3 MΩ·cm, liquid-vapor surface tension $\gamma_{LV} = 72.81$ mJ·m^{-2}) and methylene iodide (Sigma-Aldrich, Milan, Italy; liquid-vapor surface tension $\gamma_{LV} = 50.82$ mJ·m^{-2}) in air was thus measured by the sessile drop method, by gentle dropping of a 4±0.5 µL droplet of water onto the coated surface of the plastic substrate, according to the so-called pick-up procedure (whereby the droplet hanging down the needle is laid on the coating surface by raising of the sample stage until the solid/liquid contact is reached). All droplets were released from 1 cm above the surface to minimize the inconsistency between each measurement. Each analysis was replicated at least ten times, and the mean contact angles were then used for all subsequent calculations. The surface energy of the solid (γ_{SV}) was determined by the Owens and Wendt theory, using Equation (2) [32]:

$$(1 + \cos\theta)\gamma_{LV} = 2(\sqrt{\gamma_{LV}^d \gamma_{SV}^d} + \sqrt{\gamma_{LV}^p \gamma_{SV}^p}) \quad (2)$$

which is widely used for the surface characterization of low-surface energy polymers (e.g., polyolefins) [33]. Since the values of the polar (γ_{LV}^p) and dispersive (γ_{LV}^d) components of both water ($\gamma_{LV}^p = 51.0$ mJ·m^{-2}; $\gamma_{LV}^d = 21.8$ mJ·m^{-2}) and methylene iodide ($\gamma_{LV}^p = 0$ mJ·m^{-2}; $\gamma_{LV}^d = 50.8$ mJ·m^{-2}) are known, the dispersive and polar components of the solid's surface tension (γ_{SV}^d and γ_{SV}^p, respectively) can easily be drawn. Finally, the surface energy of the polyolefin surface is obtained according to Equation (3):

$$\gamma_{SV} = \gamma_{SV}^d + \gamma_{SV}^p \quad (3)$$

Atomic force microscopy (AFM)

AFM maps were collected in 'soft' contact mode stabilized by the standard optical-lever method with a very small force offset, using a commercial setup (AlphaSNOM, WITec GmbH, Germany). The height variation in the resulting topography maps is represented by a color scale, in which bright and dark colors denote higher and lower heights, respectively. The root mean square roughness R was evaluated for each sample as the standard deviation of the topography over the 95×95 µm^2 scanning area (M×N pixels), by means of Equation (4):

$$R = \sqrt{\frac{1}{MN}\sum_{i=1}^{M}\sum_{j=1}^{N}\left|z(x_i,y_j) - \overline{z}\right|^2} \quad (4)$$

where $\overline{z}$ is the mean value of the topography $z(x,y)$ [34]. The so-called 'ironed surface', i.e. the true exposed surface area, is also calculated for each map by means of a standard commercial software.

X-ray photoelectron spectroscopy (XPS)

XPS measurements were performed in an M-Probe instrument (Surface Science Instruments, USA) equipped with a monochromatic Al K$_\alpha$ source (1486.6 eV) with a spot size of 200 µm×750 µm and a pass energy of 25 eV, providing a resolution for 0.74 eV. The energy scale was calibrated with

reference to the $4f_{7/2}$ level of a freshly evaporated gold sample, at 84.0±0.1 eV, and with reference to the $2p_{3/2}$ and 3s levels of copper at 932.47±0.1 and 122.39±0.15 eV, respectively. With a monochromatic source, an electron flood gun was used to compensate for the buildup of positive charge on the insulator samples during the analyses: a value of 10 eV was selected for these samples to be measured. For all the samples, the C 1s peak level was taken as internal reference at 284.6 eV. The accuracy of the reported binding energies (BE) can be estimated to be ±0.2 eV.

3. Results and discussion
3.1. Morphology

The effect of flame treatment on the surface roughness of polyolefins has been investigated in previous studies [35]. It slightly smoothed the surface in some cases [27], while in others it had no effect [16, 36]. The different morphology of the untreated PP plaques is confirmed by the AFM images (Figure 2) and by the indices R and I_S (Table 1). The H-type sample is clearly the roughest with R ~22 times and ~2 times larger than samples S and M, respectively. The same trend was observed for the I_S index, which accounts for the total amount of exposed surface.

Visual inspection of the different AFM maps reveals that the main change in the sample topography ensuing from the flame treatments lies in the appearance of new aggregates with a size in the few-micrometer range. While such aggregates are well-rendered in Figure 2b and 2c, i.e. for the treated S sample, their presence on the treated rougher samples is partially hidden in the image by the overall large height fluctuation of the sample topography. To better visualize these aggregates, we applied a line-by-line correction by subtraction of a

7th-order fitting curve, obtaining the maps shown in Figure 3, where the presence of the small aggregates is even more evident. According to Strobel *et al.* [37], we are inclined to believe that the original topography of the PP surfaces treated with a fuel-lean flame is altered by a new physical arrangement of PP molecular chains, specifically the agglomeration and ordering of partially oxidized intermediate-molecular-weight material formed in the treatment. Therefore, the new morphology detected on the PP plaques should be considered the result of the combined effect of temperature (flattening of the original roughness) and oxidation of the PP caused by the flame (formation of new aggregates). Conversely, the formation of low-molecular-weight oxidized material (LMWOM), typical of corona-treated PP [38], should here be excluded. This is because the presence of LMWOM has been associated with extensive chain scission primarily involving atomic oxygen. However, it has been demonstrated that, during flame treatment, the concentration of O is very low relative to the concentration of OH and the other active species, which explains the lack of LMWOM [37]. This, in turn, is the main reason why flame-treated PP is more stable than corona-treated PP as a function of storage time under ambient conditions [19, 22, 39].

3.2. Wettability

In Table 2 the values of contact angles for water ($\theta_{(w)}$) and methylene iodide ($\theta_{(d)}$) and the solid-liquid surface energy (γ_{SV}) with the disperse and polar components (γ_{SV}^d, γ_{SV}^p) are reported for untreated, 1-step-treated and 2-step-treated PP samples. Figure 4 displays instead the typical water contact angle profile for an H-type PP plaque before treatment and after one and two sequential treatments. Similar to the untreated samples, the highest surface energy was measured for the smoother type (S), which also had the highest polar component (1.21 mJ·m⁻²). The lowest surface energy was instead encountered for the H-type sample, despite the higher polar component (0.32 mJ·m⁻²) compared with the M sample (0.08 mJ·m⁻²). This observation can be explained when we take into account the 'roughness effect' described by the Cassie-Baxter theory, which suggests an increase, proportional to surface roughness, in the hydrophobic attribute of inherently hydrophobic surfaces [40]. Eventually, the contribution arising from the rougher topogra-
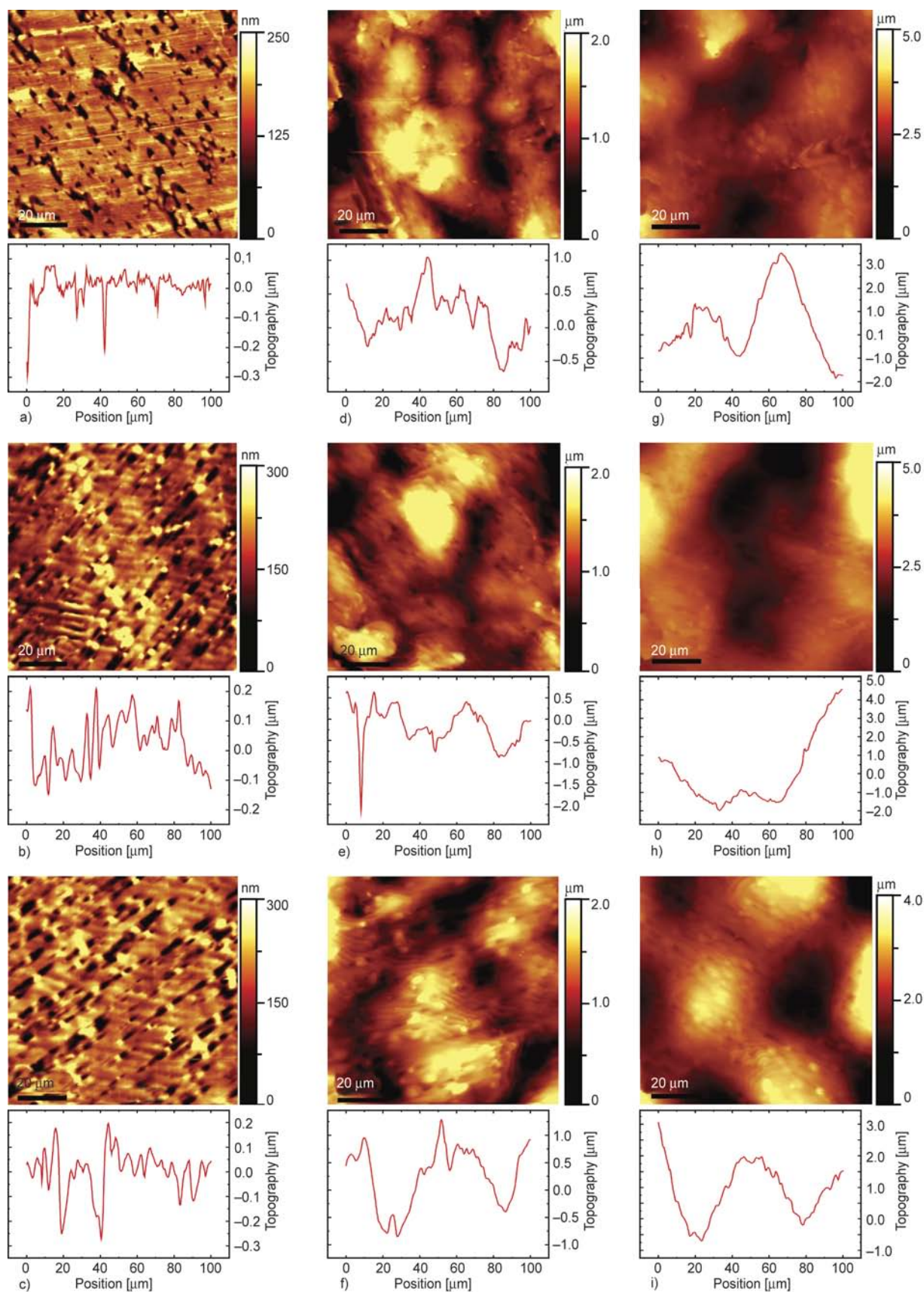
Table 1. Root mean squares roughness (R [μm]) and ironed surface (I_S [μm²]) of untreated, 1-step-treated, and 2-step-treated PP plaques at different roughness

PP type	Untreated plaques Morphological parameter		1step-treated plaques Morphological parameter		2 step-treated plaques Morphological parameter	
	R	**I_S**	**R**	**I_S**	**R**	**I_S**
S	0.06	9068	0.092	9075	0.098	9084
M	0.60	9286	0.570	9189	0.531	9165
H	1.34	9329	1.480	9197	1.184	9237

S – smooth; M – medium roughness; H – high roughness.

Figure 2. 95×95 μm² AFM height maps of samples S [first column, (a)–(c)], M [second column, (d)–(f)], and H [third column, (g)–(i)] before flame treatment (first row), after 1 step (second row), and after 2 steps (third row) flame treatment. A representative line profile is also reported below each map.
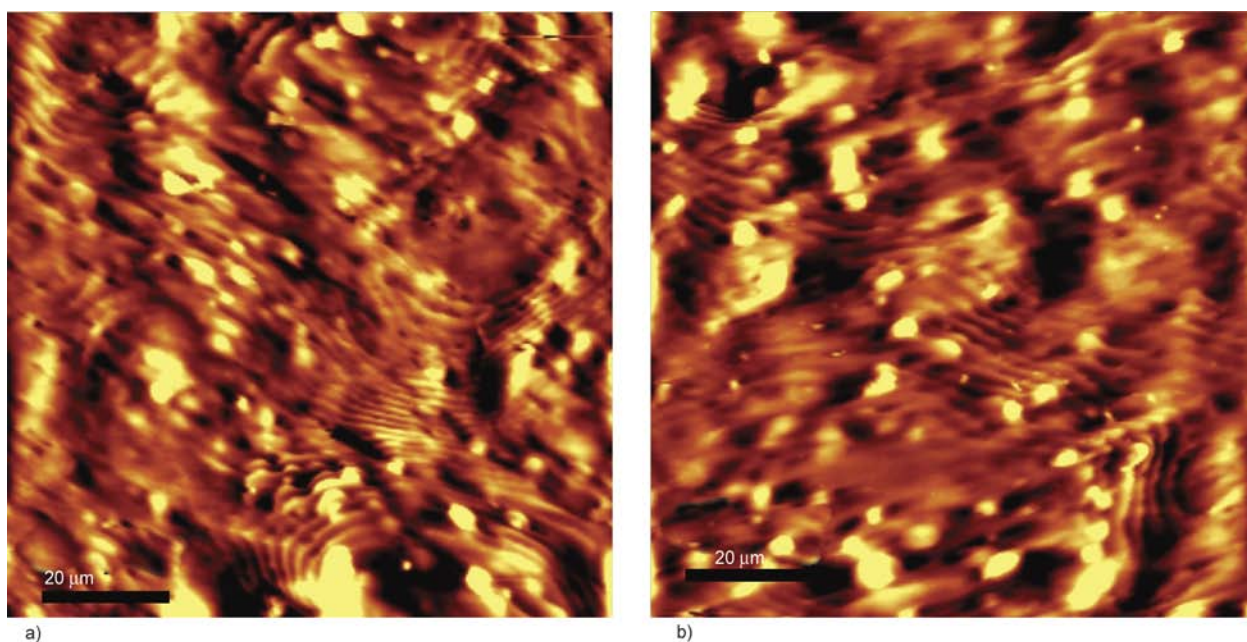
Figure 3. Corrected topography maps after 7th-order line-by-line correction of the M [panel (a)] and H [panel (b)] samples after 2 flame treatments.

Table 2. Static water (*w*) and methylene iodide (*d*) contact angles (θ [°]), solid surface energy (γ_{SV} [mJ·m^{-2}]) and its components (γ_{SV}^d and γ_{SV}^p [mJ·m^{-2}]) of untreated, 1-step-treated, and 2-step-treated PP plaques at different roughness

PP type	Untreated plaques					1-step-treated plaques					2-step-treated plaques				
	Thermodynamic parameter					Thermodynamic parameter					Thermodynamic parameter				
	$\theta_{(w)}$	$\theta_{(d)}$	γ_{SV}	γ_{SV}^d	γ_{SV}^p	$\theta_{(w)}$	$\theta_{(d)}$	γ_{SV}	γ_{SV}^d	γ_{SV}^p	$\theta_{(w)}$	$\theta_{(d)}$	γ_{SV}	γ_{SV}^d	γ_{SV}^p
S	95.40[a] ±0.99	54.28[a] ±1.53	31.89	30.68	1.21	72.38[a] ±1.65	46.46[a] ±1.26	40.65	31.41	9.24	68.57[a] ±1.46	43.90[a] ±1.30	43.16	32.21	10.95
M	104.74[b] ±1.18	56.33[b] ±1.14	31.07	30.99	0.08	74.63[b] ±1.16	47.66[a] ±1.83	39.32	31.08	8.24	68.10[a] ±2.20	43.75[a] ±1.04	43.41	32.21	11.20
H	103.75[b] ±1.29	61.34[c] ±0.99	27.91	27.59	0.32	73.32[a] ±1.54	43.22[b] ±0.95	40.67	32.14	8.54	68.12[a] ±2.68	43.68[a] ±2.07	43.42	32.25	11.17

Different letters within group (i.e., column) denote statistically significant differences between samples ($p < 0.05$).
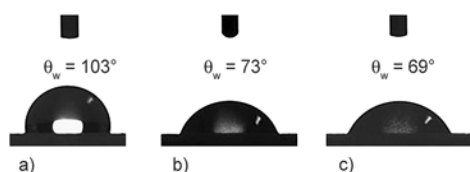

Figure 4. Typical water contact angle (θ_w) profile for an H-type PP plaque: (a) before flame treatment; (b) after one treatment; (c) after two treatments

phy of the H sample overcompensated for the effect of the higher polar component, finally yielding a higher surface energy value.

The flame's effect on the wettability attribute of the PP plaques was decidedly marked. As reported in Table 2 (dataset in the middle), the activation of the PP surface by one treatment was achieved insomuch as the water contact angle was decreased by ~24, ~29, and ~30% for the samples S, M, and H, respectively, with corresponding surface energy values of ~40 mJ·m^{-2} for all three sample types. The relevance of this result can be better understood by the consideration that the value of ~38 mJ·m^{-2} is, in most applications, the minimum surface energy value required to achieve an adequate adhesion strength between a polymeric material (e.g., plastic substrates) and the adherend (e.g., water-based adhesives, inks, paints and, more generally, coating systems).

After two treatments, the efficacy of the flame treatment in changing the PP samples' wettability properties was increased. As reported in Table 2 (last dataset on the right), contact angle values as high as ~68° were eventually obtained, which implies surface energy values of approximately 43 mJ·m^{-2}. Noticeably, the latter is a typical value recorded for more hydrophilic polymers, such as polyethylene terephthalate (PET). Not less important is the increase in the polar component of the PP surfaces ensuing

from the flame treatment, which was ~11 mJ·m^{-2} for all three types of plaques (Table 2).

3.3. Surface chemistry

Appreciation of the elemental surface composition of both untreated and flame-treated samples was gathered by XPS measurements. Untreated PP plaques exhibited a single peak related to the C 1s signal (Figure 5a). This is the non-functionalized carbon (C–C), at a binding energy (BE) of 284.7 eV

(this peak is taken as the reference peak) [41]. Neither oxygen nor nitrogen was detected (Table 3). Two-step flamed samples disclosed a different spectrum, characterized by both traces of contaminants and of the products of the flame treatment. Contaminants such as Si, F, Ca, and S arise from additives/technological aids migrated to the polymer surface. Since their contents were small and did not appreciably vary after the flame treatment, their contribution was neglected. Main peaks on the flamed sam-
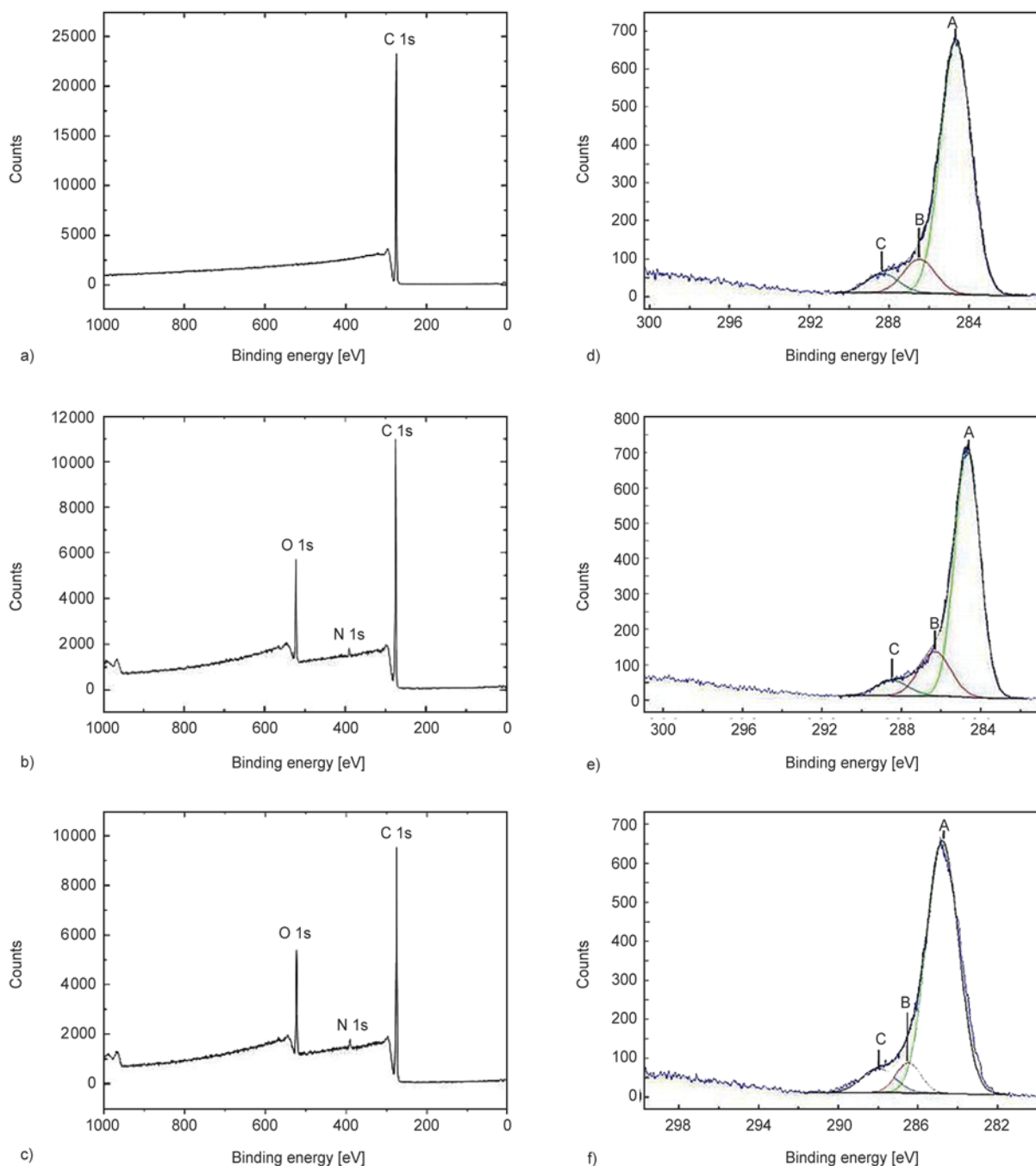
Figure 5. Left panels: raw scan spectra of untreated (a) and 2-step-treated samples S (b) and H (c); right panels: fitting of the C 1s peaks for samples S (d), M (e), and H (f)

Table 3. Elemental surface composition of polyolefin samples before and after flame treatments, determined by XPS. Note that the treated samples S, M, and H have been subjected to 2 sequential passes (interval between passes = 10 s).

Sample	C [%]	O [%]	N [%]
Untreated	100.0	–	–
S	83.7	14.1	2.2
M	83.5	14.0	2.5
H	83.3	13.8	2.9

ples were due to the functionalization of the C–C backbone by the flame's oxidizing effect. As indicated by the new peak at ~532 eV in Figure 5b (sample S) and Figure 5c (sample H), all three samples (viz. S, M, and H morphologies) experienced a marked increase in oxygen content after the treatment (~14%, see Table 3). This value is in line with those reported by Papirer *et al.* [23] for 2-step-treated PP. Further information on the type of functional groups ensuing from the oxidation of the C–C backbone can be obtained by fitting of the C 1s peak using a combination of Gaussian and Lorentzian curves.

This allowed disclosing three main components: (i) nonfunctionalized carbon (C–C) at 284.6 eV; (ii) carbon carrying hydroxyl groups (C–OH) at ~286.6±0.2 eV; and (iii) carbon involved in carbonyl groups (C=O) at ~289.0±0.2 eV [42]. These three components are respectively denoted by the letters A, B, and C, in Figures 5d–5f, for samples S, M, and H. As already reported, the insertion of these new oxygen-containing functional groups onto the C–C skeleton is responsible for the increased wettability and surface energy values of flame-treated PP plaques [43]. It appears, moreover, that most of the new polar functionalities are represented by hydroxyl species (peak denoted as B in Figures 5d–5f), confirming what was reported by Sheng *et al.* [20], who estimated that ~20–30% of the oxygen added to PP by flame treatment could be in the form of hydroxyl groups. Newly formed nitrogen was also observed (peak at ~390 eV) on the flamed samples, with an apparent increase in N content proportional to the sample's initial roughness. The presence of nitrogen-containing compounds on flame-treated PP is somehow controversial. For example, Pijpers and Meier [21] observed a significant amount of N at the surface of PP samples at air/ propane ratios between 26 and 18, whereas Papirer *et al.*

[23] and Briggs *et al.* [44] reported the appearance of N- derivatives only on flamed polyethylene (PE). The origin of N compounds is not yet well understood. On one hand, the formation of NO_x (among which nitrogen monoxide is the most abundant) could stem from the oxidation of molecular nitrogen (N_2) in combustion air. On the other hand, the presence of N derivatives has been ascribed to N-containing additives/stabilizers (e.g., Tinuvin® 770) commonly used in the manufacture of polyolefins [21]. Whatever the origin of N-derivatives, from a practical point of view it would be better to keep their formation during flaming as low as possible. This is because the formation of NO_x, which is in an inverse proportion to CH_x intermediates, would impair the surface activation of the polyolefin surface [26]. Since NO_x formation is promoted by increased temperatures, residence times, and O_2 concentrations, it can easily be controlled during treatment operations by burning under lean conditions and flame-quenching with a secondary air stream.

The surface chemistry analysis confirmed what we gathered from both AFM and contact angle measurements. The two-step treatment was sufficiently high to reset any morphological difference between samples, because of the high thermal input (heat) associated with the flame. This, in turn, allowed making void any influence arising from the surface roughness as observed in the pristine (i.e., not treated) samples. The ultimate effect was the chemical modification of the PP surfaces, which occurred to a same extent in the three sample types, as demonstrated by the XPS results.

4. Conclusions

In this work it was demonstrated that the surface topography, which greatly affects the wettability properties of bare polypropylene samples, did not affect the surface activation of the same polymer mediated by flame treatment. After one treatment, the water contact angle was dramatically reduced for both smooth and rough surfaces, although the highest polar component was still recorded for the smooth-type surface. After two treatments, however, any initial difference between samples linked to the heterogeneous morphology was apparently reset, as demonstrated by the comparable values of both surface energy and polar components. This finding may be relevant for all those applications which envisage the use of one individual polymer (such as

PP) with different morphologies (e.g., injection-molded objects). No less important, the flame treatment's efficacy was such as to raise the final surface energy of PP surfaces to ~43 mJ·m^{-2}, a value comparable to that of inherently hydrophilic/wettable polymers. This was confirmed to be due to the functionalization of the PP backbone by polar functional groups, such as hydroxyl and carbonyl groups.

References

[1] Hargittai I., Comotti A., Hargittai M.: Giulio Natta. Chemical and Engineering News, **81**, 26–28 (2003). DOI: 10.1021/cen-v081n006.p026

[2] Maier C., Calafut T. Polypropylene: The definitive user's guide and databook. William Andrews Publishing, New York (1998).

[3] Poisson C., Hervais V., Lacrampe M. F., Krawczak P.: Optimization of PE/binder/PA extrusion blow-molded films. II. Adhesion properties improvement using binder/EVA blends. Journal of Applied Polymer Science, **101**, 118–127 (2006). DOI: 10.1002/app.22407

[4] Singh R. P.: Surface grafting onto polypropylene – A survey of recent developments. Progress in Polymer Science, **17**, 251–281 (1992). DOI: 10.1016/0079-6700(92)90024-S

[5] Zhang G., Liao H., Cherigui M., Davim J. P., Coddet C.: Effect of crystalline structure on the hardness and interfacial adherence of flame sprayed poly(ether–ether–ketone) coatings. European Polymer Journal, **43**, 1077–1082 (2007). DOI: 10.1016/j.eurpolymj.2006.12.039

[6] Ozdemir M., Yurteri C. U., Sadikoglu H.: Physical polymer surface modification methods and applications in food packaging polymers. Critical Reviews in Food Science and Nutrition, **39**, 457–477 (1999). DOI: 10.1080/10408699991279240

[7] Briggs D.: Surface treatments for polyolefins. in 'Surface analysis and pretreatment of plastics and metals' (ed.: Brewis D. M.) MacMillan Publishing, New York, 199–226 (1982).

[8] Molitor P., Barron V., Young T.: Surface treatment of titanium for adhesive bonding to polymer composites: A review. International Journal of Adhesion and Adhesives, **21**, 129–136 (2001). DOI: 10.1016/S0143-7496(00)00044-0

[9] Lisboa P., Gilliland D., Ceccone G., Valsesia A., Rossi F.: Surface functionalisation of polypyrrole films using UV light induced radical activation. Applied Surface Science, **252**, 4397–4401 (2006). DOI: 10.1016/j.apsusc.2005.07.091

[10] López D., Burillo G.: Gamma-ray irradiation of polystyrene in the presence of cross-linking agents. in 'Radiation effects on polymers' (eds.: Clough R. L., Shalaby S. W.) ACS Symposium Series, Vol. 475, 262–270 (1991). DOI: 10.1021/bk-1991-0475.ch016

[11] Murray K. A., Kennedy J. E., McEvoy B., Vrain O., Ryan D., Cowman R., Higginbotham C. L.: The influence of electron beam irradiation conducted in air on the thermal, chemical, structural and surface properties of medical grade polyurethane. European Polymer Journal, **49**, 1782–1795 (2013). DOI: 10.1016/j.eurpolymj.2013.03.034

[12] Ensinger W., Müller H. R.: Surface modification and coating of powders by ion beam techniques. Materials Science and Engineering: A, **188**, 335–340 (1994). DOI: 10.1016/0921-5093(94)90389-1

[13] Slepička P., Slepičková Kasalková N., Stránská E., Bačáková L., Švorčik V.: Surface characterization of plasma treated polymers for applications as biocompatible carriers. Express Polymer Letters, **7**, 535–545 (2013). DOI: 10.3144/expresspolymlett.2013.50

[14] Wingfield J. R. J.: Treatment of composite surfaces for adhesive bonding. International Journal of Adhesion and Adhesives, **13**, 151–156 (1993). DOI: 10.1016/0143-7496(93)90036-9

[15] Strobel M., Jones V., Lyons C. S., Ulsh M., Kushner M. J., Dorai R., Branch M. C.: A comparison of corona-treated and flame-treated polypropylene films. Plasmas and Polymers, **8**, 61–95 (2003). DOI: 10.1023/A:1022817909276

[16] Strobel M., Branch M., Ulsh M., Kapaun R. S., Kirk S., Lyons C. S.: Flame surface modification of polypropylene film. Journal of Adhesion Science and Technology, **10**, 515–539 (1996). DOI: 10.1163/156856196X00562

[17] Morra M., Occhiello E., Garbassi F.: Knowledge about polymer surfaces from contact angle measurements. Advances in Colloid and Interface Science, **32**, 79–116 (1990). DOI: 10.1016/0001-8686(90)80012-O

[18] Nie H-Y., Walzak M. J., Berno B., McIntyre N. S.: Atomic force microscopy study of polypropylene surfaces treated by UV and ozone exposure: Modification of morphology and adhesion force. Applied Surface Science, **144–145**, 627–632 (1999). DOI: 10.1016/S0169-4332(98)00879-4

[19] Briggs D., Brewis D. M., Konieczko M. B.: X-ray photoelectron spectroscopy studies of polymer surfaces. Journal of Materials Science, **14**, 1344–1348 (1979). DOI: 10.1007/BF00549306

[20] Sheng E., Sutherland I., Brewis D. M., Heath R. J.: An X-ray photoelectron spectroscopy study of flame treatment of polypropylene. Applied Surface Science, **78**, 249–254 (1994).
DOI: 10.1016/0169-4332(94)90012-4

[21] Pijpers A. P., Meier R. J.: Adhesion behaviour of polypropylenes after flame treatment determined by XPS (ESCA) spectral analysis. Journal of Electron Spectroscopy and Related Phenomena, **121**, 299–313 (2001).
DOI: 10.1016/S0368-2048(01)00341-3

[22] Strobel M., Walzak M. J., Hill J. M., Lin A., Karbashewski E., Lyons C. S.: A comparison of gas-phase methods of modifying polymer surfaces. Journal of Adhesion Science and Technology, **9**, 365–383 (1995).
DOI: 10.1163/156856195X00554

[23] Papirer E., Wu D. Y., Schultz J.: Adhesion of flame-treated polyolefins to styrene butadiene rubber. Journal of Adhesion Science and Technology, **7**, 343–362 (1993).
DOI: 10.1163/156856193X00745

[24] Garbassi F., Occhiello E., Polato F., Brown A.: Surface effect of flame treatments on polypropylene. Journal of Materials Science, **22**, 1450–1456 (1987).
DOI: 10.1007/BF01233147

[25] Farris S., Piergiovanni L.: Emerging coating technologies for food and beverage packaging materials. in 'Emerging food packaging technologies: Principles and practice' (eds.: Yam K., Lee D. S.) Woodhead, Oxford, 274–302 (2012).

[26] Farris S., Pozzoli S., Biagioni P., Duó L., Mancinelli S., Piergiovanni L.: The fundamentals of flame treatment for the surface activation of polyolefin polymers – A review. Polymer, **51**, 3591–3605 (2010).
DOI: 10.1016/j.polymer.2010.05.036

[27] Mazzola L., Bemporad E., Carassiti F.: Flame treatment on plastic: A new surface free energy statistical prediction model and characterization of treated surfaces. Applied Surface Science, **257**, 2148–2158 (2011).
DOI: 10.1016/j.apsusc.2010.09.064

[28] Pitts W. M.: The global equivalence ratio concept and the formation mechanisms of carbon monoxide in enclosure fires. Progress in Energy and Combustion Science, **21**, 197–237 (1995).
DOI: 10.1016/0360-1285(95)00004-2

[29] Dillard J. G., Cromer T. F., Burtoff C. E., Cosentino A. J., Cline R. L., Maciver G. M.: Surface properties and adhesion of flame treated sheet molded composite (SMC). The Journal of Adhesion, **26**, 181–198 (1988).
DOI: 10.1080/00218468808071285

[30] Sutherland I., Brewis D. M., Health R. J., Sheng E.: Modification of polypropylene surfaces by flame treatment. Surface and Interface Analysis, **17**, 507–510 (1991).
DOI: 10.1002/sia.740170717

[31] Brewis D. M.: Pretreatments of hydrocarbon and fluorocarbon polymers. The Journal of Adhesion, **37**, 97–107 (1992).
DOI: 10.1080/00218469208031253

[32] Owens D. K., Wendt R. C.: Estimation of the surface free energy of polymers. Journal of Applied Polymer Science, **13**, 1741–1747 (1969).
DOI: 10.1002/app.1969.070130815

[33] Karbowiak T., Debeaufort F., Voilley A.: Importance of surface tension characterization for food, pharmaceutical and packaging products: A review. Critical Reviews in Food Science and Nutrition, **46**, 391–407 (2006).
DOI: 10.1080/10408390591000884

[34] Eaton P., West P.: Atomic force microscopy. Oxford University Press, Oxford (2010).

[35] Tuominen M., Ek M., Saloranta P., Toivakka M., Kuusipalo J.: The effect of flame treatment on surface properties and heat sealability of low-density polyethylene coating. Packaging Technology and Science, **26**, 201–214 (2013).
DOI: 10.1002/pts.1975

[36] Song J., Gunst U., Arlinghaus H. F., Vansco G. J.: Flame treatment of low-density polyethylene: Surface chemistry across the length scales. Applied Surface Science, **253**, 9489–9499 (2007).
DOI: 10.1016/j.apsusc.2007.06.018

[37] Strobel M., Sullivan N., Branch M. C., Jones V., Park J., Ulsh M., Strobel J. M., Lyons C. S.: Gas-phase modeling of impinging flames used for the flame surface modification of polypropylene film. Journal of Adhesion Science and Technology, **15**, 1–21 (2001).
DOI: 10.1163/156856101743283

[38] Strobel M., Dunatov C., Strobel J. M., Lyons C. S., Perron S. J., Morgen M. C.: Low-molecular-weight materials on corona-treated polypropylene. Journal of Adhesion Science and Technology, **3**, 321–335 (1989).
DOI: 10.1163/156856189X00245

[39] Strobel J. M., Strobel M., Lyons C. S., Dunatov C., Perron S. J.: Aging of air-corona-treated polypropylene film. Journal of Adhesion Science and Technology, **5**, 119–130 (1991).
DOI: 10.1163/156856191X00080

[40] Cassie A. B. D., Baxter S.: Wettability of porous surfaces. Transactions of the Faraday Society, **40**, 546–551 (1944).
DOI: 10.1039/TF9444000546

[41] Beamson G., Briggs D.: High resolution XPS of organic polymers: The Scienta ESCA300 database. Wiley, Hoboken (1992).

[42] Moulder J. F., Stickle W. F., Bomben K. D.: Handbook of X-ray photoelectron spectroscopy. Perkin Elmer, Eden Praire (1992).

[43] Alexander C. S., Branch M. C., Strobel M., Ulsh M., Sullivan N., Vian T.: Application of ribbon burners to the flame treatment of polypropylene films. Progress in Energy and Combustion Science, **34**, 696–713 (2008).
DOI: 10.1016/j.pecs.2008.04.004

[44] Briggs D., Brewis D. M., Konieczko M. B.: X-ray photoelectron spectroscopy studies of polymer surfaces. Journal of Materials Science, **11**, 1270–1276 (1976).
DOI: 10.1007/BF00545146